



OPEN Endurance exercise attenuates *Gαq-RNAi* induced hereditary obesity and skeletal muscle dysfunction via improving skeletal muscle *Srl/MRCC-I* pathway in *Drosophila*

Xin-yuan Yin✉, Deng-tai Wen✉, Han-yu Li, Zhao-qing Gao, YuZe Gao & WeiJia Hao

G protein alpha q subunit (*Gαq*) can binds to the G protein-coupled receptor (GPCR) for signaling and is closely related to lipid metabolism. Endurance exercise is an effective means of combating acquired obesity and its complications, but the mechanisms by which endurance exercise modulates hereditary obesity and its complications are unknown. In this study, we achieved knockdown of *Gαq* in drosophila adipose tissue and skeletal muscle by constructing the *Gαq-UAS-RNAi/Ppl-Gal4* and *Gαq-UAS-RNAi/Mef2-GAL4* systems. *Drosophila* were subjected a three-week endurance exercise intervention, and changes in relevant indicators were detected and observed by RT-PCR, ELISA, oil red staining, immunofluorescence staining, and transmission electron microscopy. The results showed that knockdown of *Gαq* in both adipose tissue and skeletal muscle induced a significant increase in triglycerides accompanied by a decrease in rapid climbing ability, a decrease in Superoxide Dismutase (SOD) activity level, and a decrease in Mitochondrial respiratory chain complex I (MRCC I) content in *Drosophila* whole body and skeletal muscle, and down-regulated the expression of the G protein alpha q subunit (*Gαq*), the skeletal muscle myosin heavy chain expression gene (*Mhc*), mitochondrial biogenesis gene *Spargal*(the *PGC-1alpha* homologue in *Drosophila*). Endurance exercise significantly improved the triglyceride levels in the whole body and skeletal muscle of drosophila with *Gαq* knockdown in adipose tissue and skeletal muscle, as well as their ability to climb, increased SOD activity level and MRCCI content level, and up-regulated the expression of *Gαq*, *Mhc*, and *Spargal*(*Srl*). Thus, the present findings suggest that genetic defects in the *Gαq* gene in adipose and skeletal muscle tissues induce hereditary obesity and skeletal muscle dysfunction, and that endurance exercise attenuates this hereditary obesity and concomitant skeletal muscle dysfunction in drosophila by improving skeletal muscle fiber contractile proteins, mitochondrial function and function, and antioxidant capacity via mediating the *Gαq/Mhc*, *Gαq/Srl/MRCC-I*, and *Gαq/SOD* pathways.

Keywords Endurance exercise, *Gαq* gene, Genetic obesity, Mitochondria, Skeletal muscle, *Drosophila*

The global prevalence of obesity has been increasing at an alarming rate in recent decades, seriously jeopardizing human health^{1,2}. The World Health Organization defines obesity as an abnormal or excessive accumulation of fat that poses a risk to health and is considered a global health epidemic³. Obesity is a chronic metabolic disease that is closely related to cardiovascular disease, type 2 diabetes and other chronic diseases⁴, and its causes include genetic and acquired environmental factors⁵. Some studies have shown that the acquired environment, such as high-fat/high-sucrose diets, drugs and other induced obesity can change the relevant genetic material, so that the next generation of hereditary obesity risk increases, so it is easy to form a “genetic-obesity-genetic-obesity” vicious circle⁶. Numerous studies have confirmed that endurance exercise is an effective means of combating acquired obesity and related complications^{7,8}. Its physiological mechanism lies in the fact that endurance

College of Physical Education, Ludong University, Yantai 264025, Shandong, People’s Republic of China. ✉email: 1249690988@qq.com; 191729783@qq.com

exercise can increase energy expenditure, reduce fat accumulation, improve insulin sensitivity, rebalance various metabolic and signaling pathways in the body, and attenuate the chronic inflammatory response, etc^{9–11}. However, the molecular mechanism of endurance exercise in regulating genetic obesity and its complications remains to be explored.

G protein alpha q subunit (*Gaq*) can binds to the G protein-coupled receptor (GPCR) for signaling, which is abundantly expressed in adipose, skeletal muscle and other tissues^{12,13}. *Gaq* is associated with the stimulation of insulin secretion and is often used as a drug target in the study of obesity, type 2 diabetes and other metabolic syndromes^{14–16}. It has been shown that *Gaq* can control fat storage in *Drosophila* cells and organisms, and knockdown of the adipose tissue *Gaq* gene can affect the expression of lipid metabolism effector genes, which leads to obesity in *Drosophila*¹⁷. However, whether the obesity induced by *Gaq* gene knockdown in both mammals and *drosophila* is accompanied by complications and whether it can be reversed by endurance exercise, as well as the molecular mechanisms underlying its effects, still remain to be confirmed.

Therefore, in order to determine the molecular mechanisms by which endurance exercise modulates genetic obesity and its complications, the classical genetic model organism *Drosophila* was selected for this study^{18–20}. In this study, we firstly constructed the *Gaq-UAS-RNAi/Ppl-Gal4* and *Gaq-UAS-RNAi/Mef2-GAL4* systems through *Drosophila* crosses to achieve specific knockdown of the *Gaq* gene in adipose and skeletal muscle tissues in the F1 generation, and verified whether it was successful in inducing the generation of hereditary obesity in the F1 generation through the detection of the lipid metabolism and its motility condition. Then, *Drosophila* were subjected to endurance exercise intervention, and whole body and skeletal muscle triglyceride (TG), exercise capacity, skeletal muscle SOD activity, MRCC I content, *Srl* gene, *Mhc* gene, *Gaq* gene expression level were detected. The ultrastructure, protein expression and lipid accumulation of skeletal muscle were observed by transmission electron microscopy, immunofluorescence staining and oil-red staining to comprehensively evaluate whether endurance exercise can effectively counteract obesity and concurrent skeletal muscle dysfunction caused by *Gaq* gene knockdown and reveal its molecular mechanism, so as to provide the theoretical basis and new ideas for the counteracting of hereditary obesity by endurance exercise.

Materials and methods

Drosophila strains and hybridization groups

Gaq knockdown strain w[1118] P{GD17761}v51116 (purchased from Vienna *Drosophila* Resource Center, Austria, strain number: V51116); *Ppl*^{Gal4} strain w; P{ppl-GAL4.P}2* (purchased from Bloomington *Drosophila* Stock Center, US, strain number: BCF-673); *Mef2*^{Gal4} (purchased from Bloomington *Drosophila* Stock Center, US, strain number: 27390); The F1 generation UAS/Gal4 system was constructed by crossing *Gaq*^{UAS-RNAi} with *Ppl*^{Gal4} and *Mef2*^{Gal4} *Drosophila*, respectively, to regulate the expression of the target gene *Gaq* in adipose tissue and skeletal muscle.

Male *Drosophila* within 12 h of feathering of the F1 generation of *Gaq-UAS-RNAi* male and female self-crosses were used as genetic controls and divided into the *Gaq* gene normal expression group (*Gaq*^{UAS-RNAi-C}), and the *Gaq* gene normal expression sport group (*Gaq*^{UAS-RNAi-E}); Male *Gaq-UAS-RNAi* *Drosophila* were crossed with female *Ppl*^{Gal4} *Drosophila*, and male *Drosophila* within 12 h of F1 generation feathering were collected and divided into the *Gaq* adipose tissue knockdown group (*Gaq*×*Ppl*^{RNAi-C}), and the *Gaq* adipose tissue knockdown exercise group (*Gaq*×*Ppl*^{RNAi-E}); Male *Gaq-UAS-RNAi* *Drosophila* were crossed with female *Mef2*^{Gal4} *Drosophila*, and male *Drosophila* within 12 h of F1 generation feathering were collected and divided into the *Gaq* skeletal muscle knockdown group (*Gaq*×*Mef2*^{RNAi-C}), and the *Gaq* skeletal muscle knockdown motor group (*Gaq*×*Mef2*^{RNAi-E}) (Fig. 1). All *Drosophila* were placed in an environmental culture at a constant temperature of 25 °C, 50% constant humidity, and a 12-h day/night cycle.

Exercise training

Upward climbing endurance training was performed on an exercise platform utilizing the anti-gravity climbing characteristic of *Drosophila* (Fig. 2). The principle is that the test tube is fixed on the test tube clamp, at this time the test tube is perpendicular to the ground, the bottom of the test tube *Drosophila* climbing to the top of the test tube, the test tube is automatically turned over 180° (the test tube is rotated at a speed of 60 rad/s speed uniformly), the *Drosophila* back to the bottom of the test tube to continue to climb the movement, so on and so forth. The weight of *Drosophila* was its own weight when climbing, 20 *Drosophila* per tube, 8 cm was reserved from the medium at the bottom of the test tube to the lower end of the cotton plug for the movement area of *Drosophila*, and the *Drosophila* had 10s time to perform the climbing movement each time after turning over to the bottom of the test tube. The exercise group started the training intervention from 1 day of age until the end of 3 weeks of age, with 15 min of exercise-5 min of rest lasting four times a day, and continued training for 5 days a week with 2 days of rest (Table 1).

Preparation of *Drosophila* culture medium

The culture medium preparation for *Drosophila* was based on the standard diet of *Drosophila* in previous studies²¹. Configure 1 L of *Drosophila* culture medium. Add 42 g of corn flour, 10 g of soybean flour, 13 g of yeast powder, and 8 g of agar strips to a pot, add 1 L of pure water and stir well. Stir continuously during heating to melt the agar strips thoroughly until the solution boils. Stop heating after boiling, add 31 g of sucrose and 31 g of maltose during cooling, and after sucrose and maltose are fully dissolved, add 2000 µl of preservative propionic acid and 1 g of sodium benzoate, and immediately dispense in clean culture tubes with a thickness of about 0.5 cm per tube after thorough stirring.

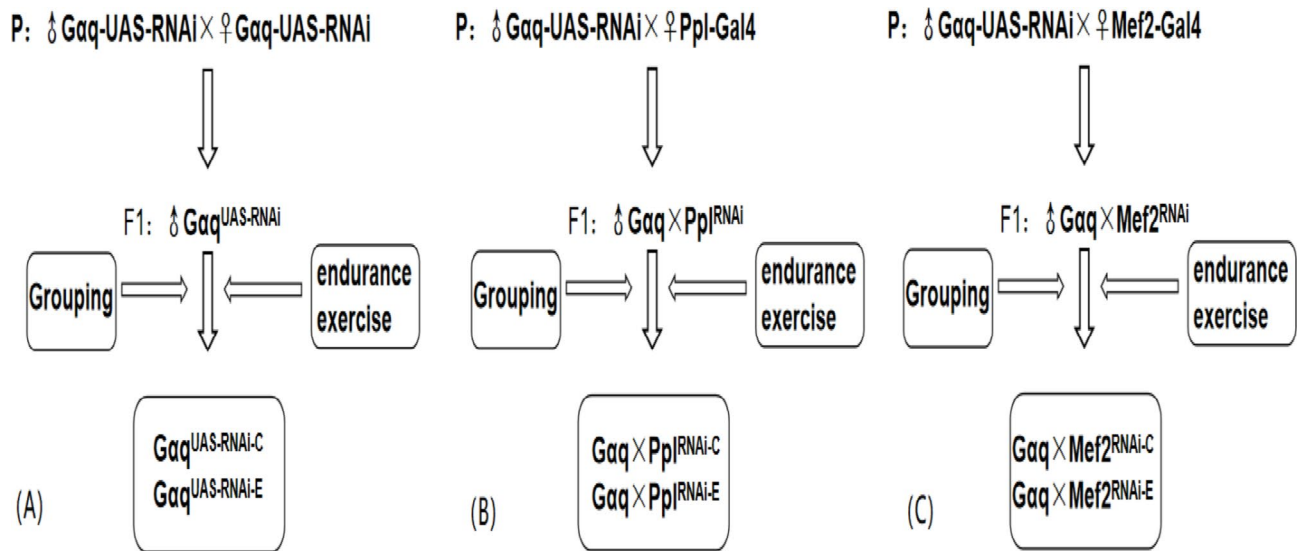


Fig. 1. Diagram of *Drosophila* hybridization and grouping. (A) *Gaq* normal expression grouping diagram. (B) *Gaq* adipose tissue knock-down grouping diagram. (C) *Gaq* skeletal muscle tissue knockdown grouping diagram.

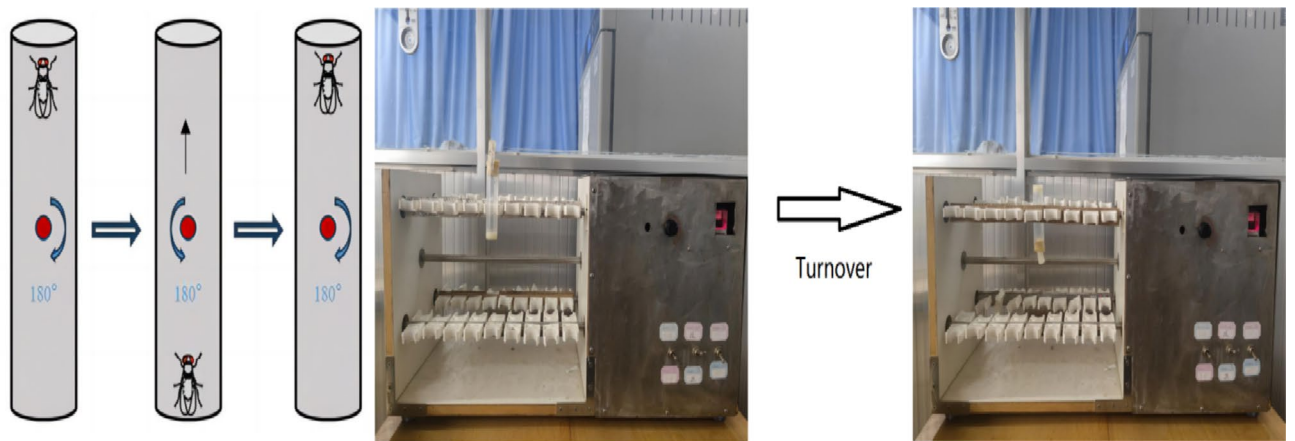


Fig. 2. Schematic diagram of *Drosophila* exercise platform and climbing training.

	Monday	Tuesday	Wednesday	Thursday	Friday	Saturday	Sunday
1st week of age	E	E	E	E	E	N	Measure climbing ability
2nd week of age	E	E	E	E	E	N	Measure climbing ability
3rd week of age	E	E	E	E	E	N	Measure climbing ability

Table 1. Exercise flow chart. E for exercise intervention, N for no exercise intervention.

ELISA assay

The activities and levels of triglyceride (TG), superoxide dismutase (SOD) and mitochondrial respiratory chain Complex I (MRCCI) in skeletal muscle of *Drosophila* were detected by using insect TG enzyme-linked immunoassay kit, insect SOD enzyme-linked immunoassay kit and insect MRCCI enzyme-linked immunoassay kit (Insect MRCCI, SOD, and TG ELISA Kits, Fankew, Shanghai Kexing Trading Co., Ltd, China). The ELISA assay-specific steps are as follows: (1) Sample addition of standard products. (2) Sample addition: Prepare blank control wells and sample wells to be tested. Add 40 μ l of diluent to the sample wells to be tested, and then add 10 μ l of test sample. (3) Add enzyme: Add enzyme-labeled reagent 100 μ l per hole, except blank hole. (4) Incubation: After the sealing plate is sealed with sealing plate film, it is incubated at 37 $^{\circ}$ C for 60 min. (5) Mixing liquid: Dilute 20 times concentrated washing liquid with 20 times distilled water for reserve use. (6)

Wash: Remove the sealing film from the surface of the sealing plate, pour out the solution in it, clean it, and then let it dry. (7) Color development: Add color-developing agent A50 μ l to each well first, then add color-developing agent B 50 μ l, gently shake and mix, and hide from light for 15 min at 37 °C. (8) Termination: Add termination solution 50 μ l per well to terminate the reaction (at this time, the blue immediately turns to yellow). (9) Determination: Determine the absorbance (OD) of each well.

Real-time quantitative PCR

At the end of three weeks of age, 50 *Drosophila* skeletal muscle (thorax) and adipose tissue (abdomen) were taken from each group and placed into 1000 μ l of Trizol respectively to detect the expression levels of relevant pathway genes. (1) Total RNA extraction: Take the homogenizer tube, add 1 ml of RNA extraction solution, place it on ice for pre-cooling, take 100 mg of tissue, add it into the homogenizer tube, and grind it fully with the grinder until no tissue mass is visible. Centrifuge at 12,000 rpm at 4 °C for 10 min, white precipitate at the bottom of the tube is RNA. Remove the liquid, add 1.5 ml of 75% ethanol for washing and precipitation, centrifuge at 12,000 rpm at 4 °C for 5 min, remove the liquid, put the centrifuge tube on a super-clean table for 3 min, add 15 μ l Water Nuclease to dissolve RNA Free, and incubate at 55 °C for 5 min. Nanodrop 2000 was used to detect RNA concentration and purity: After blank zero adjustment of the instrument, 2.5 μ l RNA solution to be tested was put on the detection base, the sample arm was lowered, and the software on the computer was used to start the absorption value detection, and the RNA with excessive concentration was diluted in an appropriate proportion so that the final concentration was 100–500 ng/ μ l. (2) Reverse transcription: Configure the reverse transcription reaction system, gently mix and centrifuge, and set the reverse transcription program. (3) Quantitative PCR: 0.2 ml PCR tubes were used to prepare the reaction system. Each retro product was prepared with 3 tubes for PCR amplification. (4) Results treatment: CT method. Primer sequences of Rp-49 were as follows: F:5'-3'CTAAGCTGTCGCACAAATGG, R:5'-3'AACTTCTTGAATCCGGTGGG; Primer sequences of *Gaq* were as follows: S:5'-3':GGTCCTCAGCGAGATGCAATAA, A:5'-3':TAAGGTTTCGATTGCAGAATTG TGTC; Primer sequences of *Mhc* were as follows: S:5'-3':GACCGTCCGTAACGATAACTCC, A:5'-3':GA CTG CTGGGAGATGA CACGA; Primer sequences of *Srl* were as follows: S:5'-3':ACCTGGCGATTCTGATTATGA C T, A:5'-3':CCTTTA CATTGTCCACATAGCGT.

Transmission electron microscopy of the skeletal muscle

For electron microscopic analysis, muscles were dissected in an ice-cold fixative (2.5% glutaraldehyde in 0.1 mol/L PIPES buffer at pH7.4). After 10 h of fixation at 4 °C, samples were washed with 0.1 mol/L PIPES, post-fixed in 1% OsO₄ (30 min), and stained in 2% uranyl acetate (1 h). Samples were dehydrated in an ethanol series (50%, 70%, 100%) and embedded in epoxy. The slices were observed and photographed with a HT-7700 transmission electron microscope.

Oil red staining analysis of skeletal muscle

Skeletal muscle was taken and fixed in tissue fixative for 15 min, rinsed with water and dried. 6 parts of saturated oil red O dye solution and 4 parts of distilled water were mixed well and placed in a water bath at 60–70 °C for 30 min, cooled naturally and then filtered through a qualitative filter paper to obtain oil red O working solution. Immerse the sections in the oil red dye solution for 8–10 min (cover to avoid light). Remove the slices, leave them for 3 s, and then immerse them sequentially in two vats of 60% isopropyl alcohol for differentiated 3 s and 5 s. Immerse the slices in two vats of pure water for 10 s each. The slices were removed, left for 3s, and immersed in hematoxylin for 3–5 min before being immersed in three tanks of pure water for 5s, 10s, and 30s, respectively. Differentiation solution was differentiated for 2–8 s, and each of the two tanks of distilled water was washed for 10s, and the blue solution was washed for 1s. The slices were gently immersed into two tanks of tap water for 5s and 10s, respectively, and examined for staining effect under the microscope. Glycerol gelatin was used to seal the sections, and the images were captured and analyzed with a microscope. Microscopy, image acquisition, and analysis: Orthostatic light microscope. Using a numerical aperture (NA) of 1.3, select an oil immersion objective measuring 40 \times . A high-resolution digital camera is attached to capture clear images to accurately measure and record details at a scale of 5 μ m. Observation is aided by a 10 \times low magnification objective that helps locate the target area quickly at the beginning of the observation and helps understand the overall distribution of the sample.

Myosin heavy chain immunofluorescence

Drosophila skeletal muscle was taken for immunohistochemical analysis as follows. (1) Paraffin sections deparaffinised to water: Put the slices in 3 changes of xylene, 10 min each, then dehydrate in 3 changes of pure ethanol for 5 min each, wash in distilled water. (2) Antigen repair: During the repair process, excessive evaporation of buffer solution should be prevented, and the slides should not be dried. After the repair is completed, it is naturally cooled. Put the slide 5 min PBS (PH 7.4) and shake it on a decoloring shaker for 3 times, each time for 5 min. (3) Circle drawing and blocking: Add 3%BSA into the circle and cover the tissue evenly to block non-specific binding at room temperature for 30 min. (The primary antibody is blocked with 10% donkey serum from goat, and the primary antibody from other sources is blocked with 3%BSA). (4) Adding primary antibody: drop the prepared primary antibody, slice it flat in a wet box and incubate at 4 °C overnight. (5) Add secondary antibody: put the glass slide 5 min PBS (PH7.4) and shake it on the decoloring shaker for 3 times, 5 min each time. Add the corresponding secondary antibody and incubate at room temperature for 50 min in the dark. (6) DAPI counterstain in nucleus: DAPI solution was dripped into the circle and incubated at room temperature for 10 min in the dark. (7) Quench tissue autofluorescence: The slides were put 5 min PBS (PH 7.4) and washed on a decoloring shaker for 3 times, each time for 5 min. Add autofluorescence quencher B solution for 5 min and rinse with running water for 10 min. (8) Mount: coverslip with anti-fade mounting

medium. (9) Microscopy detection and collect images by Fluorescent Microscopy. DAPI glows blue by UV excitation wavelength 330–380 nm and emission wavelength 420 nm; 488 glows green by excitation wavelength 465–495 nm and emission wavelength 515–555 nm; CY3 glows red by excitation wavelength 510–560 nm and emission wavelength 590 nm.

Athletic ability testing

100 *Drosophila* were randomly selected from each group, 20 per tube. Each tube was individually placed under a high definition video camera in preparation for video recording. After the camera was switched on, the *Drosophila* in the tube were shaken to the bottom of the tube every 15 s, and after three shakes, the *Drosophila* being tested was replaced with the next tube *Drosophila*. The best of three crawls of each test tube *Drosophila* was selected for data processing. Screenshots of the height of climb 3 s after *Drosophila* shocked off the bottom of the test tube were taken using AVS Video Editor software. The photo clearly shows the climbing height of the *Drosophila*. The 3-second climbing heights of the fruit flies were then processed and analysed using HEYEAR software and prism software.

Statistical methods

For comparisons of the *Gaq* gene between the *Gaq* normal expression group and the adipose tissue *Gaq* knockdown group and the skeletal muscle tissue *Gaq* knockdown group, one-way analysis of variance (ANOVA) and the least significant difference (LSD) test were used to determine between-group differences. For comparisons between control and exercise groups, independent samples t-tests were used to determine between-group differences. The experimental data were expressed as mean \pm standard deviation (S) and the significance level was taken as $\alpha = 0.05$ (or 0.01).

Results

Gaq knockdown in *Drosophila* adipose and skeletal muscle tissues induces abnormal lipid metabolism and reduced exercise capacity

Our previous studies agree that *Gaq* gene knockdown in adipose tissue induces obesity¹⁷, but its effect on exercise capacity is unknown. We first constructed a model of *Gaq* knockdown in *Drosophila* adipose tissue. The results show that compared with the *Gaq*^{UAS-RNAi-C} group, the mRNA expression level of the *Gaq* gene in *Drosophila* adipose tissue was reduced in the *Gaq* \times *Ppl*^{RNAi-C} group ($P < 0.01$) (Fig. 3A), with a relative expression rate of 43.10%. It can be judged that the *Gaq* adipose tissue knockdown model was constructed successfully. The rapid climbing ability (CS) of *Drosophila* was decreased in the *Gaq* \times *Ppl*^{RNAi-C} group ($P < 0.01$) (Fig. 3F); and the analysis of lipid by oil red staining accumulation revealed an increase in triglyceride accumulation in the skeletal muscle of *Drosophila* in the *Gaq* \times *Ppl*^{RNAi-C} group (Fig. 3G). ELISA assay of *Drosophila* in the *Gaq* \times *Ppl*^{RNAi-C} group revealed an increase in whole-body and skeletal muscle TG content ($P < 0.01$) (Fig. 3B,C), and a decrease in the level of SOD activity ($P < 0.05$) (Fig. 3D), and a decrease in the level of MRCCI ($P < 0.01$) (Fig. 3E).

To further understand that *Gaq* knockdown leads to abnormal lipid metabolism and reduced exercise capacity, we also constructed a *Drosophila* skeletal muscle tissue *Gaq* knockdown model. The results showed that compared with the *Gaq*^{UAS-RNAi-C} group, the mRNA expression level of the *Gaq* gene in *Drosophila* skeletal muscle tissue was reduced in the *Gaq* \times *Mef2*^{RNAi-C} group ($P < 0.01$) (Fig. 4A), with a relative expression rate of 66%; it can be judged that the *Gaq* skeletal muscle tissue knockdown model was constructed successfully. CS was decreased in *Drosophila* from the *Gaq* \times *Mef2*^{RNAi-C} group ($P < 0.05$) (Fig. 4F); oil-red staining analysis of lipid accumulation revealed an increase in the *Gaq* \times *Mef2*^{RNAi-C} group *Drosophila* skeletal muscle triglyceride accumulation was increased (Fig. 4G). ELISA assay of *Drosophila* in the *Gaq* \times *Mef2*^{RNAi-C} group revealed an increase in whole-body and skeletal muscle TG content ($P < 0.01$) (Fig. 4B,C), and a decrease in the level of SOD activity ($P < 0.01$) (Fig. 4D), and a decrease in the level of MRCC I ($P < 0.01$) (Fig. 4E). RT-PCR assay showed decreased mRNA expression level of skeletal muscle myosin heavy chain expression gene (*Mhc*) ($P < 0.01$) (Fig. 4H); myosin heavy chain immunofluorescence plots showed that myosin heavy chain expression was decreased in *Drosophila* skeletal muscle tissues of the *Gaq* \times *Mef2*^{RNAi-C} group, which indicated an increase in skeletal muscle damage (Fig. 4I). RT-PCR assay showed decreased mitochondrial biogenesis gene *Spargal* (*Srl*) expression was decreased ($P < 0.01$) (Fig. 4J). Skeletal muscle transmission electron microscopy images showed that *Drosophila* skeletal muscle tissues of the *Gaq* \times *Mef2*^{RNAi-C} group had disorganized myofibril arrangement and incomplete Z-lines, which indicated a weakening of skeletal muscle function (Fig. 4K).

Endurance exercise effectively improves abnormal lipid metabolism and decreased exercise capacity induced by *Gaq* knockdown

A growing body of evidence confirms that endurance exercise can effectively improve obesity and enhance exercise capacity. Therefore, we firstly performed endurance exercise intervention on *Gaq* normal expression *Drosophila*. The results showed that compared with the *Gaq*^{UAS-RNAi-C} group, there was no significant difference in the mRNA expression levels of the *Gaq* gene in the *Gaq*^{UAS-RNAi-E} group ($P > 0.05$) (Fig. 5A); CS was enhanced in *Drosophila* from the *Gaq*^{UAS-RNAi-E} group (Fig. 5F); analysis of lipid accumulation by oil-red staining showed that *Drosophila* from the *Gaq*^{UAS-RNAi-E} group lipid accumulation decreased (Fig. 5G); ELISA showed a decrease ($P < 0.01$) in their whole body and skeletal muscle TG content ($P < 0.01$) (Fig. 5B,C), and an increase in SOD activity level and MRCC I content (Fig. 5D,E).

We also performed an endurance exercise intervention on *Gaq* adipose tissue knockdown *Drosophila* melanogaster. The result shows that compared with the *Gaq* \times *Ppl*^{RNAi-C} group, the mRNA expression level of the *Gaq* gene in *Drosophila* adipose tissue was increased in the *Gaq* \times *Ppl*^{RNAi-E} group ($P < 0.01$) (Fig. 6A), and the relative expression rate was elevated by 27%; *Drosophila* CS was increased in the *Gaq* \times *Ppl*^{RNAi-E} group (Fig. 6F); oil red staining analysis of lipid accumulation showed that in the *Gaq* \times *Ppl*^{RNAi-E} group *Drosophila* skeletal

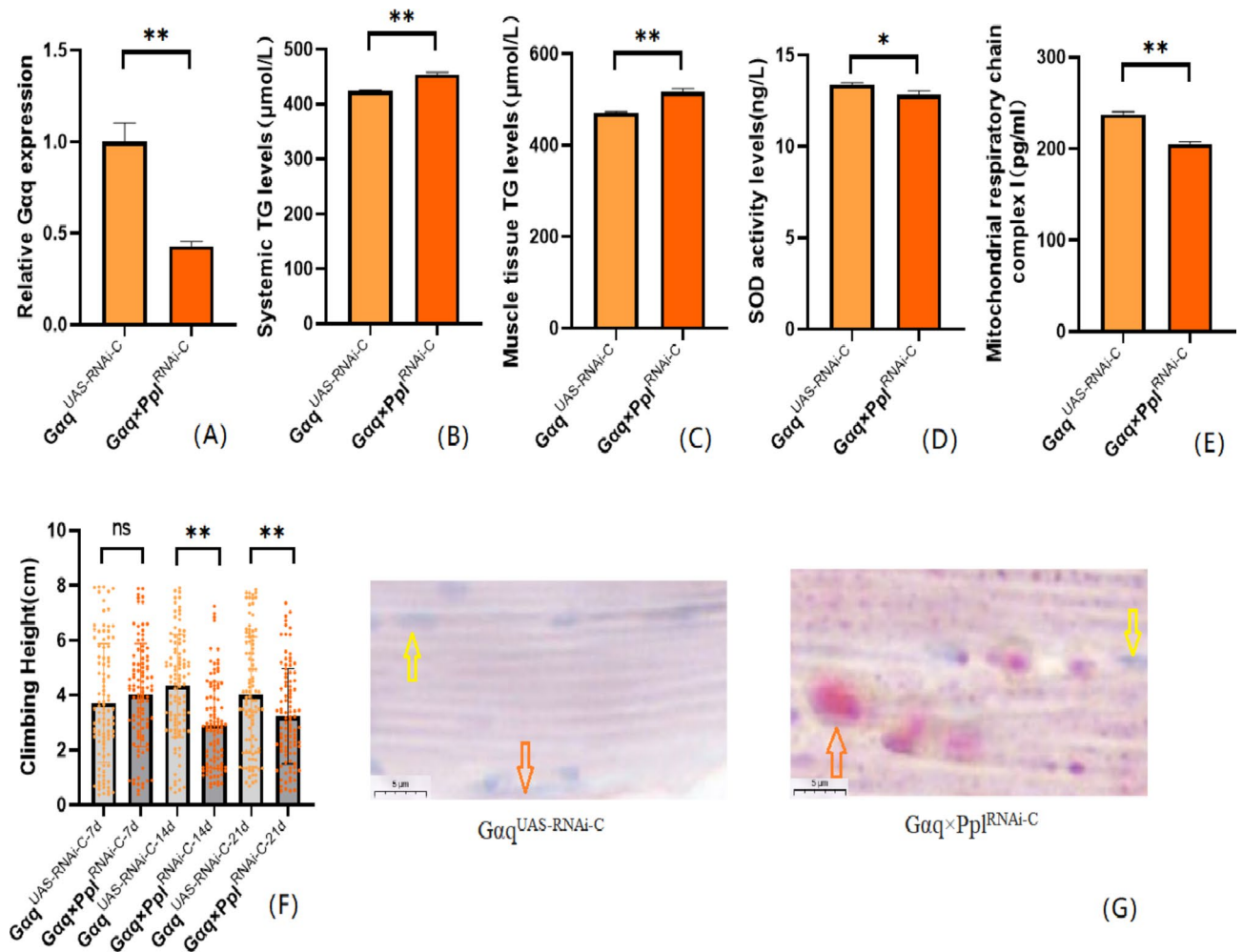


Fig. 3. Relative gene expression, lipid metabolism levels, oxidative capacity, mitochondrial function, and 3s climbing ability in adipose-tissue *Gaq* knockdown *Drosophila* skeletal muscle. **(A)** Relative expression of *Gaq*, Sample $n = 50$. **(B)** Whole Body Triglyceride Levels, Sample $n = 20$. **(C)** Skeletal muscle tissue triglyceride levels, Sample $n = 30$. **(D)** SOD activity levels, Sample $n = 30$. **(E)** Mitochondrial respiratory chain complex I content, Sample $n = 30$. **(F)** Climbing height, Sample $n = 100$. **(G)** Oil red staining, Sample $n = 5$. Yellow arrows indicate nuclei and orange arrows indicate lipid accumulation (scale: black line is 5 μm). The one-way analysis of variance (ANOVA) with least significant difference (LSD) tests was used to identify difference among the groups. Data are represented as mean \pm standard deviation. * $P < 0.05$; ** $P < 0.01$; n s means no significant difference.

muscle tissue showed decreased lipid accumulation (Fig. 6G); ELISA detected decreased levels of systemic and skeletal muscle TG ($P < 0.01$) (Fig. 6B,C), increased levels of SOD activity ($P < 0.05$) (Fig. 6D), and increased MRCC I content ($P < 0.01$) (Fig. 6E).

We also performed endurance exercise intervention on *Gaq* skeletal muscle tissue knockdown *Drosophila*. The result shows that compared with the *Gaq* \times *Mef2*^{RNAi-C} group, the mRNA expression level of the *Gaq* gene was elevated in the skeletal muscle tissue of *Drosophila* in the *Gaq* \times *Mef2*^{RNAi-E} group ($P < 0.05$) (Fig. 7A), and the relative expression rate was elevated by 13.67%; and the CS of *Drosophila* in the *Gaq* \times *Mef2*^{RNAi-E} group was increased ($P < 0.01$) (Fig. 7F); Oil red staining analysis of lipid accumulation showed a decrease in lipid accumulation in the skeletal muscle tissue of *Drosophila* in the *Gaq* \times *Mef2*^{RNAi-E} group (Fig. 7G), and a decrease in the TG content of its whole body and skeletal muscle as detected by ELISA ($P < 0.01$) (Fig. 7B,C), and an increase in the level of SOD activity (Fig. 7D), and the content of MRCC I ($P < 0.01$) (Fig. 7E); immunofluorescence images of myosin heavy chain showed increased expression of myosin heavy chain in *Drosophila* skeletal muscle tissues of the *Gaq* \times *Mef2*^{RNAi-E} group, indicating reduced muscle damage and enhanced muscle function (Fig. 7I), and RT-PCR showed elevated levels of *Mhc* expression ($P < 0.05$) (Fig. 7H); transmission electron microscopy images of skeletal muscle showed that *Drosophila* of the *Gaq* \times *Mef2*^{RNAi-E} group skeletal muscle myogenic fibres are more aligned and Z-lines are more complete, indicating enhanced muscle function (Fig. 7K), and RT-PCR showed elevated *Srl* expression level ($P < 0.05$) (Fig. 7J).

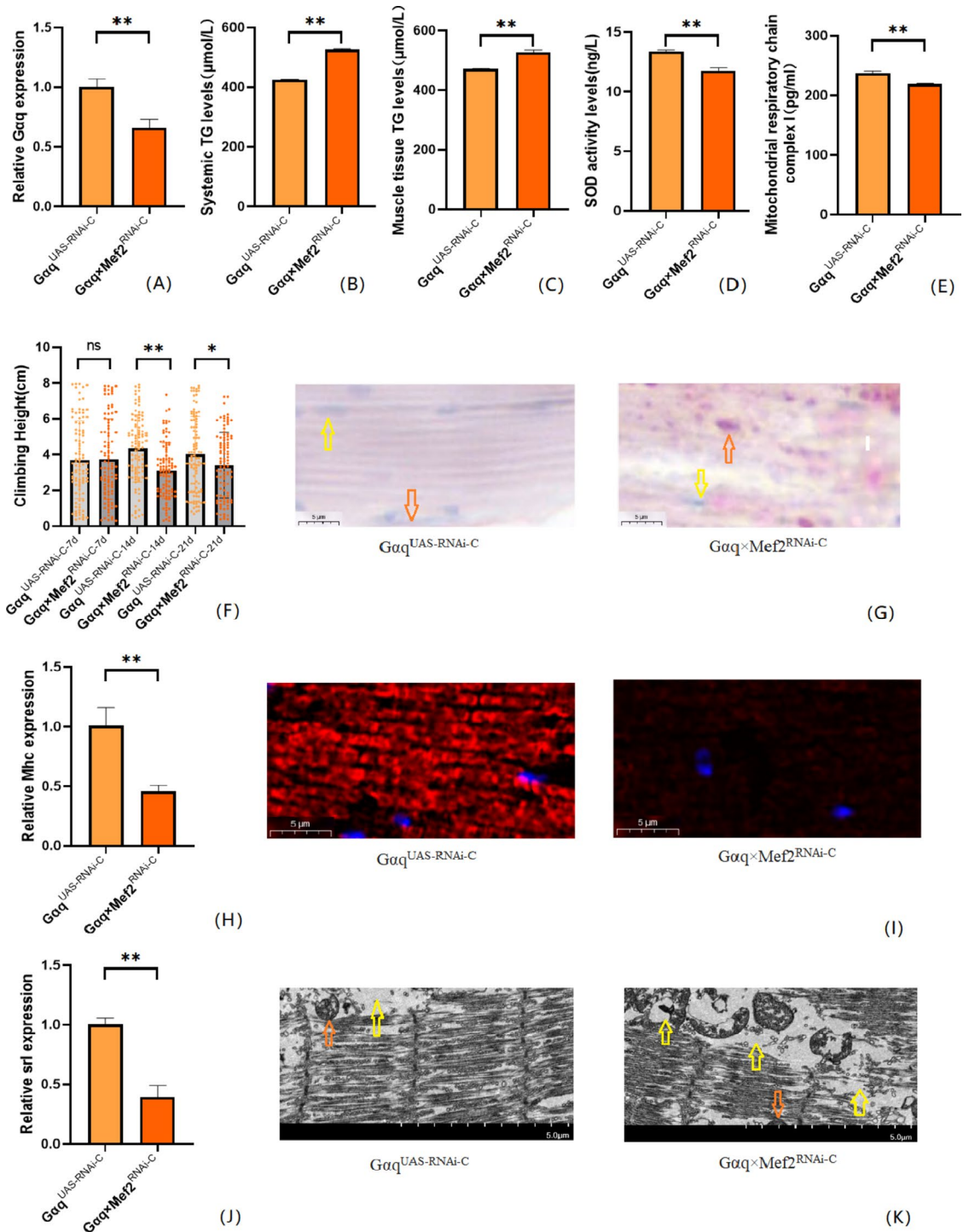


Fig. 4. Relative gene expression, lipid metabolism levels, oxidative capacity, mitochondrial function, and 3 s climbing ability in skeletal muscle tissue *Gaq* knockdown of *Drosophila* skeletal muscle. (A) Relative expression of *Gaq*, Sample $n = 50$. (B) Whole Body Triglyceride Levels, Sample $n = 20$. (C) Muscle Tissue Triglyceride Levels, Sample $n = 30$. (D) SOD activity levels, Sample $n = 30$. (E) Mitochondrial respiratory chain complex I content, Sample $n = 30$. (F) Climbing height, Sample $n = 100$. (G) Oil red staining, Sample $n = 5$. Yellow arrows indicate nuclei and orange arrows indicate lipid accumulation (scale: black line is 5 μm). (H) Relative expression of *Mhc*, Sample $n = 50$. (I) Immunofluorescence image of myosin heavy chain, Sample $n = 5$, blue dots are nuclei and red fluorescent bands are myogenic fibers (scale: white line is 5 μm). (J) Relative expression of *Srl*, Sample $n = 50$. (K) Transmission electron micrograph of skeletal muscle, Sample $n = 5$, orange indicates nuclei, yellow indicates muscle fiber damage (scale, white line is 5 μm). The one-way analysis of variance (ANOVA) with least significant difference (LSD) tests was used to identify difference among the groups. Data are represented as mean \pm standard deviation. * $P < 0.05$; ** $P < 0.01$; n s means no significant difference.

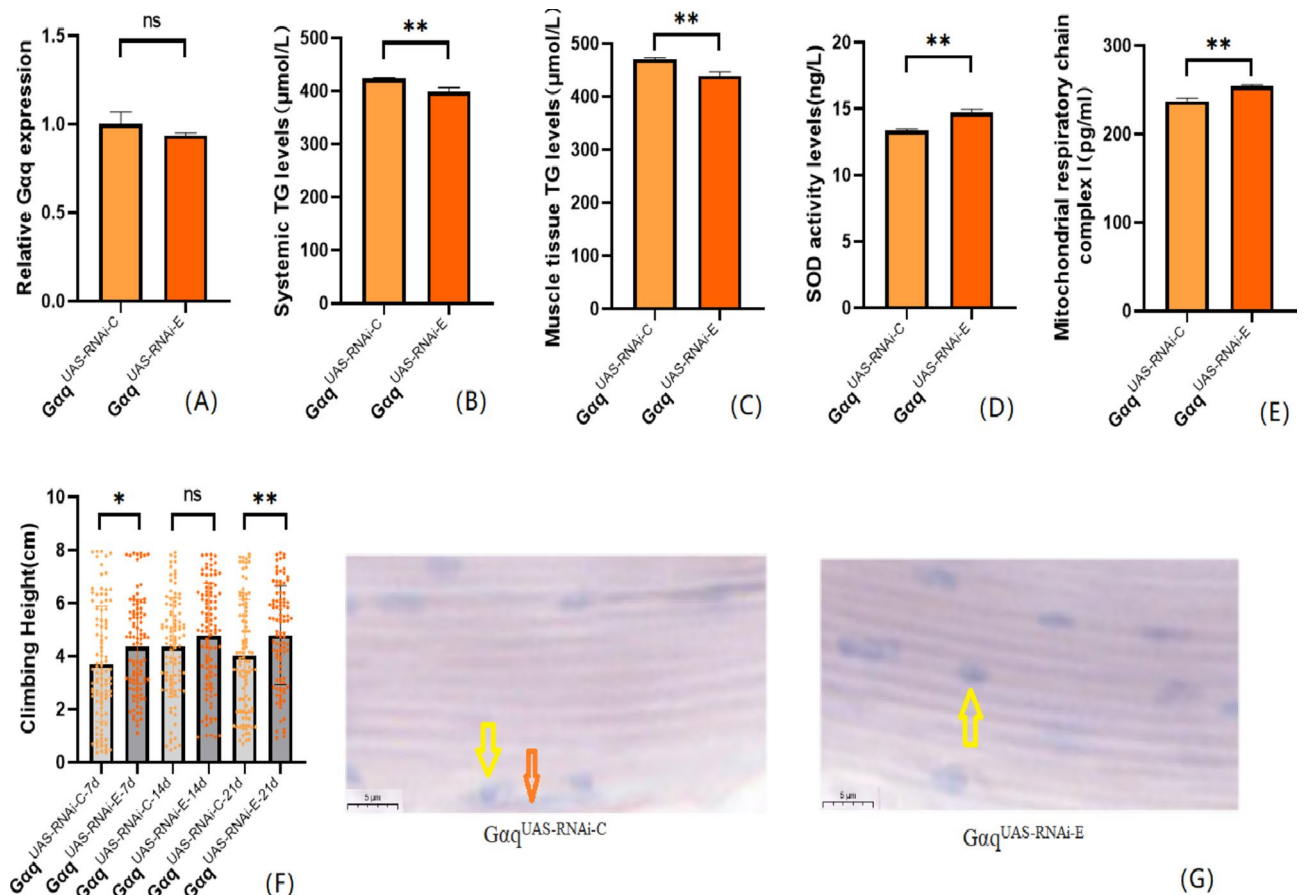


Fig. 5. After endurance exercise intervention, *Gaq* normally expressed related gene expression, lipid metabolism level, oxidation capacity, mitochondrial function and 3s climbing ability of *Drosophila melanogaster*. (A) Relative expression of *Gaq*, Sample $n = 50$. (B) Whole Body Triglyceride Levels, Sample $n = 20$. (C) Muscle Tissue Triglyceride Levels, Sample $n = 30$. (D) SOD activity levels, Sample $n = 30$. (E) Mitochondrial respiratory chain complex I content, Sample $n = 30$. (F) Climbing height, Sample $n = 100$. (G) Oil red staining, Sample $n = 5$. Yellow arrows indicate nuclei and orange arrows indicate lipid accumulation (scale: black line is 5 μm). The one-way analysis of variance (ANOVA) with least significant difference (LSD) tests was used to identify difference among the groups. Data are represented as mean \pm standard deviation. * $P < 0.05$; ** $P < 0.01$; n s means no significant difference.

Discussion

Numerous studies have reported that G protein alpha q subunit (*Gaq*) is closely related to lipid metabolism²². Recent studies have found significant changes in mRNA encoding G protein-coupled receptors (GPCR) in obese populations^{23,24}. *Gaq* directly or indirectly regulates lipid, glucose metabolism, and fat thermogenesis in adipose, liver, and muscle tissues^{25,26}. In addition, *Gaq* can also regulate fat storage, and knocking down the *Gaq* gene in adipose tissue can lead to obesity in *Drosophila*¹⁷. In this study, we successfully constructed knockdown models of *Gaq* in *Drosophila* adipose tissue and skeletal muscle tissue using the *Gaq-UAS/Ppl-Gal4* and *Gaq-UAS/Mef2-Gal4* systems. We found that genetic knockdown of the *Gaq* gene in adipose tissue and skeletal muscle resulted in an increase in triglycerides throughout the body and skeletal muscle of *Drosophila*, suggesting the possibility of inducing obesity. Meanwhile, research has found that genetic knockdown of the *Gaq* gene in adipose tissue and skeletal muscle tissue is accompanied by a significant decrease in the rapid climbing ability of *Drosophila*, suggesting that obesity may lead to skeletal muscle dysfunction.

Myosin is an important skeletal muscle contraction protein, and mitochondria are the energy “factory” of skeletal muscle. Both are closely related to skeletal muscle function. The expression of myosin and mitochondrial synthase in mammals is regulated by multiple genes, while *Drosophila* have gene expression of single skeletal muscle fiber myosin heavy chain and mitochondrial synthase^{27–29}. Both in mammals and *Drosophila*, high-fat diet induced obesity can lead to a decrease in their motor ability, which is related to the weakened functions of *Mhc* and *PGC-1alpha*. In addition, age-related skeletal muscle atrophy is also associated with the decline of skeletal muscle contraction proteins and mitochondrial function^{30–32}. Numerous studies have shown that obesity is accompanied by increased lipid toxicity in important organs such as the heart and skeletal muscle. The mechanism behind this is that under oxidative stress, lipids can form malondialdehyde (MDA), which can produce cytotoxicity and impair their function^{33–37}.

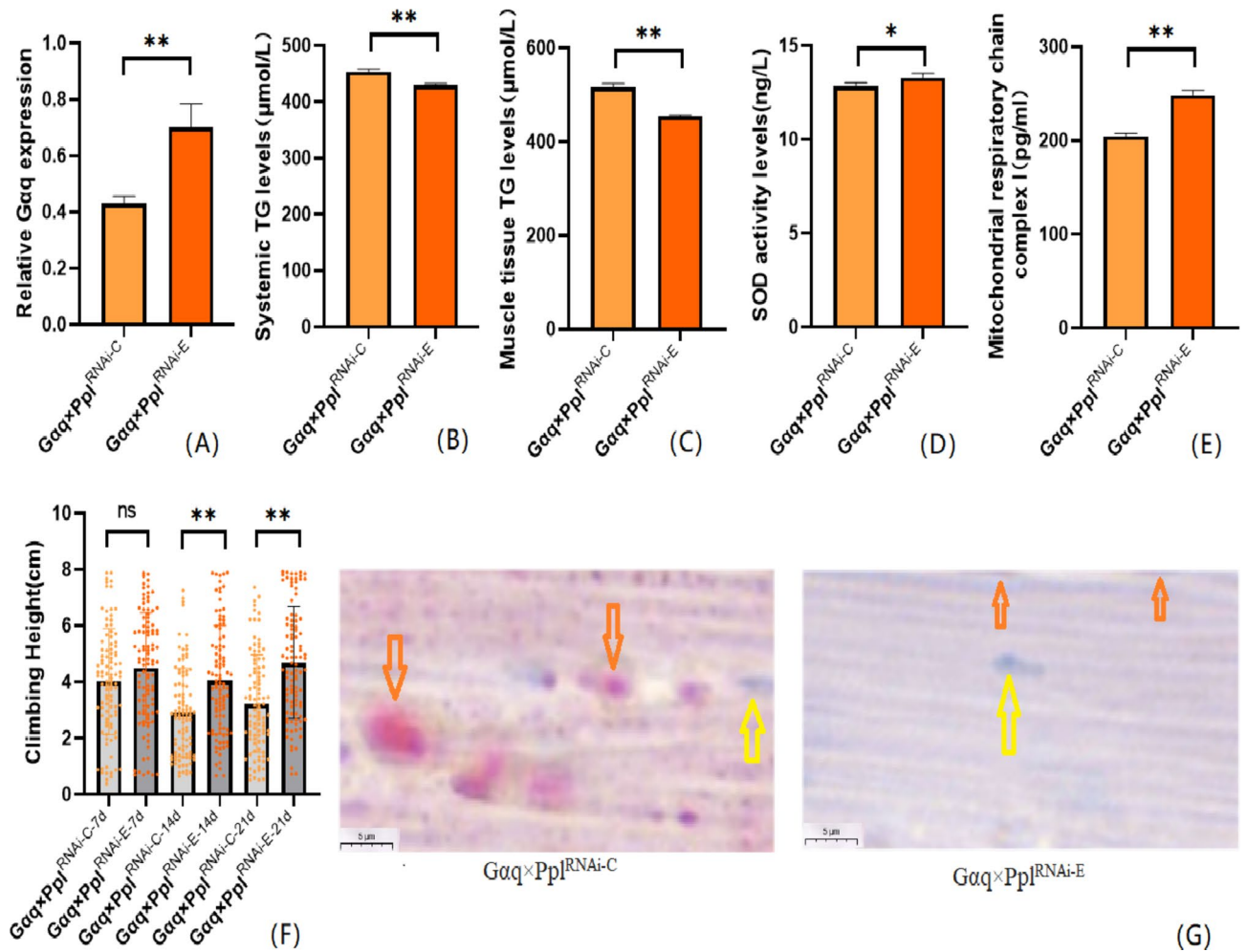


Fig. 6. After endurance exercise intervention, adipose tissue *Gaq* knockdown *Drosophila* related gene expression, lipid metabolism level, oxidation capacity, mitochondrial function and 3 s climbing ability. (A) Relative expression of *Gaq*, Sample $n = 50$. (B) Whole Body Triglyceride Levels, Sample $n = 20$. (C) Muscle Tissue Triglyceride Levels, Sample $n = 30$. (D) SOD activity levels, Sample $n = 30$. (E) Mitochondrial respiratory chain complex I content, Sample $n = 30$. (F) Climbing height, Sample $n = 100$. (G) Oil red staining, Sample $n = 5$. Yellow arrows indicate nuclei, orange arrows indicates lipid accumulation (scale: black line is 5 μm). The one-way analysis of variance (ANOVA) with least significant difference (LSD) tests was used to identify difference among the groups. Data are represented as mean \pm standard deviation. * $P < 0.05$; ** $P < 0.01$; ns means no significant difference.

To further verify the causes of skeletal muscle dysfunction, in this study, we analyzed the contractile proteins, mitochondrial status, and antioxidant capacity of skeletal muscle. The results showed that genetic knockdown of the *Gaq* gene in adipose tissue and skeletal muscle tissue can significantly reduce the expression of the important contraction protein myosin heavy chain gene (*Mhc*) and protein in skeletal muscle. At the same time, electron microscopy observation revealed a regular arrangement and reduced quantity of myofibrils. In addition, the levels of key genes *Spargel* (the *PGC-1alpha* homologue in *Drosophila*) and mitochondrial key oxidase mitochondrial respiratory chain complex I (MRCC I) involved in mitochondrial biogenesis were significantly reduced. Finally, the activity level of SOD, an important antioxidant enzyme, was detected, and it was found that genetic knockdown of *Gaq* gene in both adipose tissue and skeletal muscle tissue could reduce SOD activity level in skeletal muscle. Therefore, these results suggest that genetic knockdown of *Gaq* gene in both adipose tissue and skeletal muscle can negatively affect the important contractile structure, mitochondrial function, and antioxidant capacity of skeletal muscle, resulting in decreased exercise ability of *Drosophila*.

Endurance exercise is a globally recognized weight loss method, but whether it still has an effect on different types of obesity (especially genetic obesity induced by different gene mutations) remains to be studied^{38,39}. In rats and *Drosophila*, studies have found that endurance exercise enhances antioxidant capacity to protect them from the decline in climbing ability caused by high-fat intake, and can improve obesity caused by excessive triglyceride accumulation in the body due to high-fat diet^{21,40,41}. Recent studies have confirmed that endurance exercise can also promote mitochondrial biogenesis, aerobic capacity, and energy utilization, activate oxidative metabolism related pathways, and improve skeletal muscle metabolism and function⁴²⁻⁴⁴.

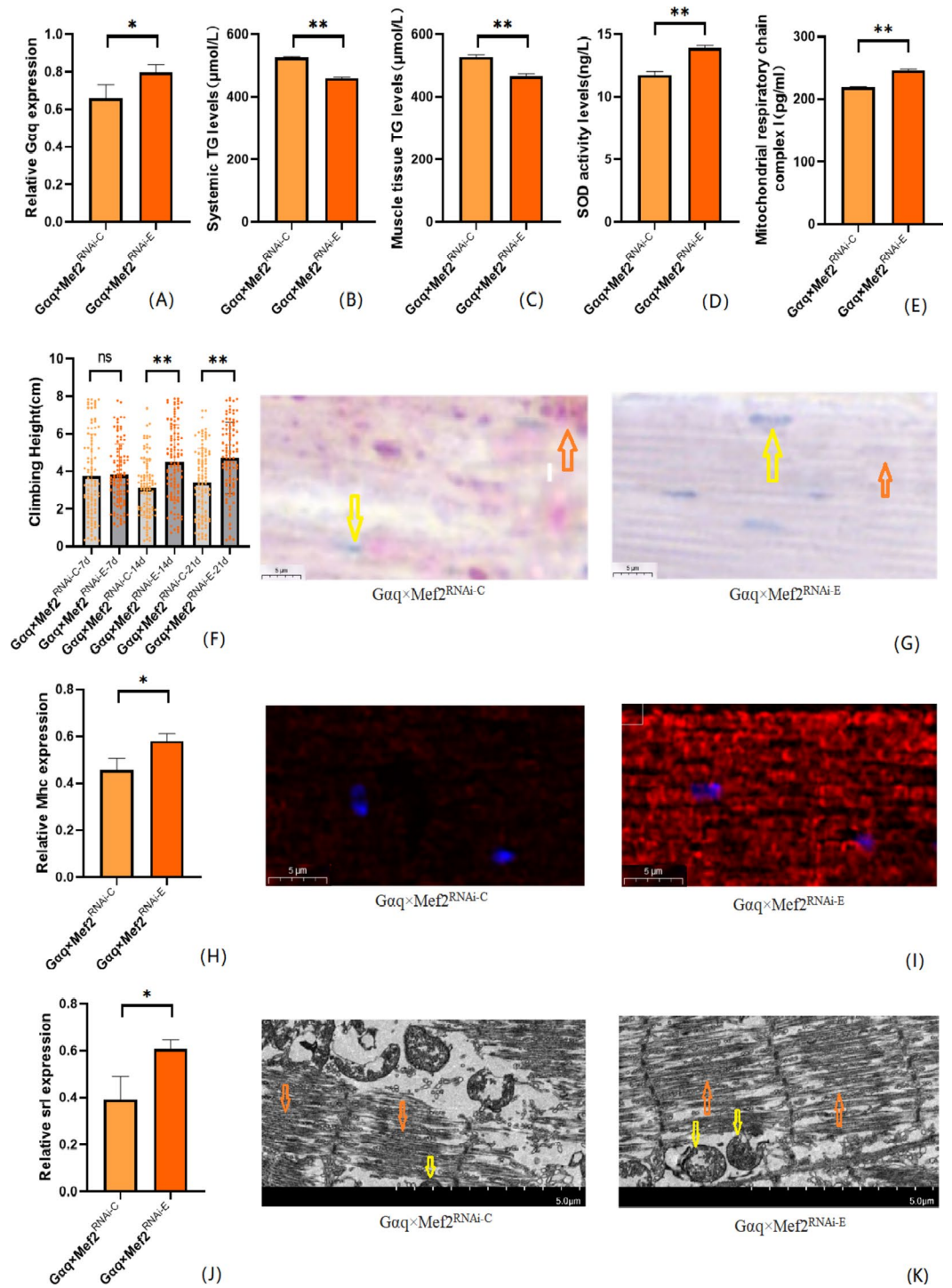


Fig. 7. After endurance exercise intervention, skeletal muscle tissue *Gaq* knockdown *Drosophila* *Drosophila* related gene expression, lipid metabolism level, oxidation capacity, mitochondrial function and 3s climbing ability. (A) Relative expression of *Gaq*, Sample $n = 50$. (B) Whole body triglyceride levels, sample $n = 20$. (C) Muscle Tissue Triglyceride Levels, Sample $n = 30$. (D) SOD activity levels, Sample $n = 30$. (E) Mitochondrial respiratory chain complex I content, Sample $n = 30$. (F) Climbing height, Sample $n = 100$. (G) Oil red staining, Sample $n = 5$. Yellow arrows indicate nuclei and orange arrows indicate lipid accumulation (scale: black line is $5 \mu\text{m}$). (H) Relative expression of *Mhc*, Sample $n = 50$. (I) Immunofluorescence image of myosin heavy chain, Sample $n = 5$, blue dots are nuclei and red fluorescent bands are myogenic fibers (scale: white line is $5 \mu\text{m}$). (J) Relative expression of *Srl*, Sample $n = 50$. (K) Transmission electron micrograph of skeletal muscle, Sample $n = 5$, yellow arrows represent mitochondria and the orange arrows represent myofibril. (scale, white line is $5 \mu\text{m}$). The one-way analysis of variance (ANOVA) with least significant difference (LSD) tests was used to identify difference among the groups. Data are represented as mean \pm standard deviation. * $P < 0.05$; ** $P < 0.01$; ns means no significant difference.

Similarly, in this study, in order to verify whether endurance exercise can produce positive benefits on obesity and concurrent motor disability induced by genetic knockdown of *Gaq* in adipose tissue and skeletal muscle tissue, we conducted endurance exercise intervention for 3 weeks in *Drosophila* with genetic knockdown of *Gaq* in adipose tissue and skeletal muscle tissue. The results showed that endurance exercise significantly increased the expression of *Gaq* gene in adipose tissue and skeletal muscle tissue of *Drosophila*, and was accompanied by a significant decrease in TG levels in the whole body and skeletal muscle, suggesting that endurance exercise plays an important role in the regulation of *Gaq* gene and its mediated obesity. In addition, behavioral indicators showed that endurance exercise could enhance the fast climbing ability of *Drosophila* with *Gaq* knockdown in adipose tissue and skeletal muscle tissue, and physiological and biochemical indicators showed that endurance exercise significantly increased the expression of *Mhc* gene and protein in skeletal muscle of *Drosophila* with *Gaq* gene knockdown in adipose tissue and skeletal muscle tissue. At the same time, electron microscopy observed that myogenic fibres were more aligned, indicating enhanced muscle function. In addition, after exercise intervention, the levels of *Spargel(Srl)* and MRCC I in skeletal muscle were significantly increased, indicating enhanced mitochondrial function. Finally, it was also found that the SOD activity level of skeletal muscle was significantly increased after exercise, suggesting that the antioxidant capacity of skeletal muscle was enhanced.

Long term exercise training, whether in mammals or *Drosophila*, can cause adaptive changes in certain gene proteins in skeletal muscle tissue cells, thereby improving their function. Research has shown that structural abnormalities of *Mhc* protein in skeletal muscle can significantly reduce exercise capacity⁴⁵. Elevated expression of *Srl*(homologue of *PGC-1 α*) in skeletal muscle can limit muscle atrophy, while reduced expression of *Srl* gene specificity leads to decreased exercise capacity and increased fat accumulation. Stimulating the *Sirt1-Srl* axis can improve motor function and mitochondrial respiratory capacity in patients with Babbitt syndrome^{46,47}. Exercise can restore the expression of *Mhc* protein mRNA in skeletal muscle of diabetes rats to normal⁴⁸. Exercise can also delay skeletal muscle aging by increasing the activities of *Sirt1/Srl* pathway and FOXO/SOD pathway^{49,50}. Similar to previous research results, this study found that endurance exercise can reduce obesity by upregulating the expression of *Gaq* genes in skeletal muscle and adipose tissue. At the same time, endurance exercise can improve the skeletal muscle structure and function of *Drosophila* with *Gaq* gene knockdown in skeletal muscle and adipose tissue by mediating the regulation of *Gaq/Mhc*, *Gaq/Srl/MRCC-I*, and *Gaq/SOD* pathways in three aspects: skeletal muscle contraction protein, mitochondria function, and antioxidant capacity, enhancing their exercise ability (Fig. 8).

Conclusion

Genetic defects in the adipose tissue and skeletal muscle tissue *Gaq* genes induce hereditary obesity and skeletal muscle dysfunction in *Drosophila*. In addition, endurance exercise positively regulates the adipose tissue and skeletal muscle tissue *Gaq* genes and improves skeletal muscle fiber contractile proteins, mitochondrial function, and antioxidant capacity, thereby attenuating this genetic obesity and concomitant skeletal muscle dysfunction.

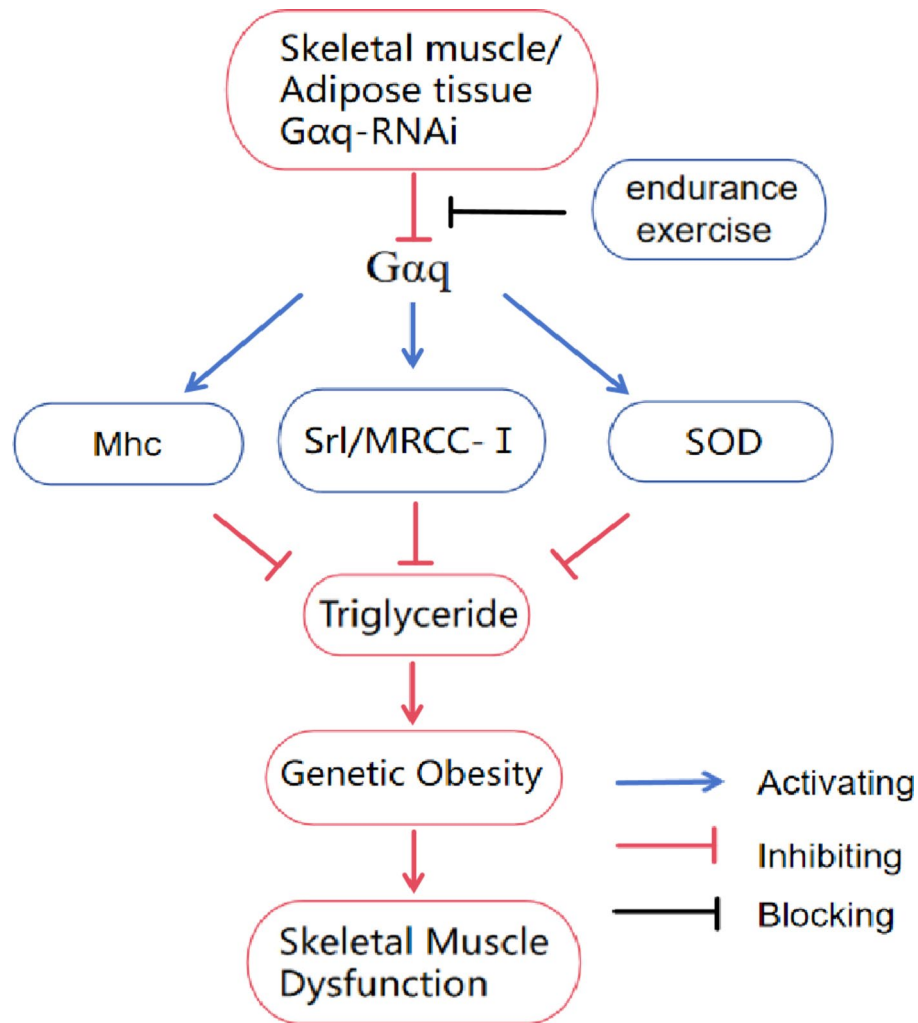


Fig. 8. Relationship between Gaq gene and endurance exercise and genetic obesity and skeletal muscle dysfunction. Gaq-RNAi in muscle and adipose tissue inhibits the Gaq mediated Gaq/Mhc, Gaq/Srl/MRCC-I, and Gaq/SOD pathways, leading to increased triglyceride accumulation in F1 Drosophila, inducing genetic obesity and further developing skeletal muscle dysfunction. This process can be blocked by endurance exercise.

Data availability

All the generated data and the analysis developed in this study are included in this article.

Received: 12 August 2024; Accepted: 8 November 2024

Published online: 15 November 2024

References

- Koliaki, C., Dalamaga, M. & Liatis, S. Update on the obesity epidemic: After the sudden rise, is the upward trajectory beginning to flatten? *Curr. Obes. Rep.* **12**(4), 514–527. <https://doi.org/10.1007/s13679-023-00527-y> (2023).
- Shabana, H. S. Obesity more than a ‘cosmetic’ problem. Current knowledge and future prospects of human obesity genetics. *Biochem. Genet.* <https://doi.org/10.1007/s10528-015-9700-2> (2020).
- Manzo, R. et al. Environmental enrichment prevents gut dysbiosis progression and enhances glucose metabolism in high-fat diet-induced obese mice. *Int. J. Mol. Sci.* **25**(13), 6904. <https://doi.org/10.3390/ijms25136904> (2024).
- Manikat, R. & Nguyen, M. H. Nonalcoholic fatty liver disease and non-liver comorbidities. *Clin. Mol. Hepatol.* **29**(Suppl), 86–102. <https://doi.org/10.3350/cmh.2022.0442> (2023).
- Sandoval-Bórquez, A. et al. Adipose tissue dysfunction and the role of adipocyte-derived extracellular vesicles in obesity and metabolic syndrome. *J. Endocr. Soc.* **8**(8), bvae126. <https://doi.org/10.1210/jendso/bvae126> (2024).
- Dearden, L. et al. Maternal obesity increases hypothalamic mir-505-5p expression in mouse offspring leading to altered fatty acid sensing and increased intake of high-fat food. *PLoS Biol.* **22**(6), e3002641. <https://doi.org/10.1371/journal.pbio.3002641> (2024).
- Lin, J. et al. Exercise ameliorates muscular excessive mitochondrial fission, insulin resistance and inflammation in diabetic rats via irisin/AMPK activation. *Sci. Rep.* **14**(1), 10658. <https://doi.org/10.1038/s41598-024-61415-6> (2024).
- Cao, Y. et al. Regular exercise in Drosophila prevents age-related cardiac dysfunction caused by high fat and heart-specific knockdown of Skd. *Int. J. Mol. Sci.* **24**(2), 1216. <https://doi.org/10.3390/ijms24021216> (2023).

9. Kolnes, K. J., Petersen, M. H., Lien-Iversen, T., Højlund, K. & Jensen, J. Effect of exercise training on fat loss-energetic perspectives and the role of improved adipose tissue function and body fat distribution. *Front. Physiol.* **12**, 737709. <https://doi.org/10.3389/fphys.2021.737709> (2021).
10. Sharma, S., Thibodeau, S. & Lytton, J. Signal pathway analysis of selected obesity-associated melanocortin-4 receptor class V mutants. *Biochim. Biophys. Acta Mol. Basis Dis.* **1866**(8), 165835. <https://doi.org/10.1016/j.bbdis.2020.165835> (2020).
11. Yan, H. et al. Regular exercise modulates the dfoxo/dsrebP pathway to alleviate high-fat-diet-induced obesity and cardiac dysfunction in *Drosophila*. *Int. J. Mol. Sci.* **24**(21), 15562. <https://doi.org/10.3390/ijms242115562> (2023).
12. Lin, C. Y. et al. Leu27 IGF-II-induced hypertrophy in H9c2 cardiomyoblasts is ameliorated by saffron by regulation of calcineurin/NFAT and CaMKII δ signaling. *Environ. Toxicol.* **36**(12), 2475–2483. <https://doi.org/10.1002/tox.23360> (2021).
13. Pedroni, L. et al. Free fatty acid receptors beyond fatty acids: a computational journey to explore peptides as possible binders of GPR120. *Curr. Res. Food Sci.* **8**, 100710. <https://doi.org/10.1016/j.crf.2024.100710> (2024).
14. Bone, D. B. J. et al. Skeletal muscle-specific activation of Gq signaling maintains glucose homeostasis. *Diabetes* **68**(6), 1341–1352. <https://doi.org/10.2337/db18-0796> (2019).
15. Grunddal, K. V. et al. Selective release of gastrointestinal hormones induced by an orally active GPR39 agonist. *Mol. Metab.* **49**, 101207. <https://doi.org/10.1016/j.molmet.2021.101207> (2021).
16. Lattanzi, R. et al. MRAP2 inhibits β -Arrestin-2 recruitment to the Prokineticin receptor 2. *Curr. Issues Mol. Biol.* **46**(2), 1607–1620. <https://doi.org/10.3390/cimb46020104> (2024).
17. Baumbach, J., Xu, Y., Hehlert, P. & Kühnlein, R. P. Gq, G γ 1 and Plc21C control *Drosophila* body fat storage. *J. Genet. Genom.* **41**(5), 283–292. <https://doi.org/10.1016/j.jgg.2014.03.005> (2014).
18. Mora, I., Puiggròs, F., Serras, F., Gil-Cardoso, K. & Escoté, X. Emerging models for studying adipose tissue metabolism. *Biochem. Pharmacol.* **223**, 116123. <https://doi.org/10.1016/j.bcp.2024.116123> (2024).
19. Hou, W. Q. et al. Physical exercise ameliorates age-related deterioration of skeletal muscle and mortality by activating Pten-related pathways in *Drosophila* on a high-salt diet. *FASEB J.* **37**(12), e23304. <https://doi.org/10.1096/fj.202301099R> (2023).
20. Yu, S. et al. Inonotus obliquus aqueous extract inhibits intestinal inflammation and insulin metabolism defects in *Drosophila*. *Toxicol. Mech. Methods* **13**. <https://doi.org/10.1080/15376516.2024.2368795> (2024).
21. Wang, J. F., Wen, D. T., Wang, S. J., Gao, Y. H. & Yin, X. Y. Muscle-specific overexpression of Atg2 gene and endurance exercise delay age-related deteriorations of skeletal muscle and heart function via activating the AMPK/Sirt1/PGC-1 α pathway in male *Drosophila*. *FASEB J.* **37**(11), e23214. <https://doi.org/10.1096/fj.202301312R> (2023).
22. Balapattabi, K. et al. Angiotensin AT1A receptor signal switching in Agouti-related peptide neurons mediates metabolic rate adaptation during obesity. *Cell. Rep.* **42**(8), 112935. <https://doi.org/10.1016/j.celrep.2023.112935> (2023).
23. Lyu, Z., Zhao, M., Atanes, P. & Persaud, S. J. Quantification of changes in human islet G protein-coupled receptor mRNA expression in obesity. *Diabet. Med.* **39**(12), e14974. <https://doi.org/10.1111/dme.14974> (2022).
24. Cui, Y., Auclair, H., He, R. & Zhang, Q. GPCR-mediated regulation of beige adipocyte formation: implications for obesity and metabolic health. *Gene* **915**, 148421. <https://doi.org/10.1016/j.gene.2024.148421> (2024).
25. Rahbani, J. F. et al. ADRA1A-Gq signalling potentiates adipocyte thermogenesis through CKB and TNAP. *Nat. Metab.* **4**(11), 1459–1473. <https://doi.org/10.1038/s42255-022-00667-w> (2022).
26. Zhang, X. & Macielag, M. J. GPR120 agonists for the treatment of diabetes: a patent review (2014 present). *Expert Opin. Ther. Pat.* **30**(10), 729–742. <https://doi.org/10.1080/13543776.2020.1811852> (2020).
27. Voss, A. C. et al. Exercise microdosing for skeletal muscle health applications to spaceflight. *J. Appl. Physiol.* **136**(5), 1040–1052. <https://doi.org/10.1152/jappphysiol.00491.2023> (2024).
28. Chiles, J. W. et al. Differentially co-expressed myofibre transcripts associated with abnormal myofibre proportion in chronic obstructive pulmonary disease. *J. Cachexia Sarcopenia Muscle* **15**(3), 1016–1029. <https://doi.org/10.1002/jcsm.13473> (2024).
29. Vaziri, P., Ryan, D., Johnston, C. A. & Cripps, R. M. A novel mechanism for activation of myosin regulatory light chain by protein kinase C-delta in *Drosophila*. *Genetics* **216**(1), 177–190. <https://doi.org/10.1534/genetics.120.303540> (2020).
30. Yang, S. H. et al. Fermented yak-kong using *Bifidobacterium animalis* derived from Korean infant intestine effectively relieves muscle atrophy in an aging mouse model. *Food Funct.* **30**. <https://doi.org/10.1039/d3fo04204a> (2024).
31. Lawler, J. M. & Hindle, A. Living in a box or call of the wild? Revisiting lifetime inactivity and sarcopenia. *Antioxid. Redox Signal.* **15**(9), 2529–2541. <https://doi.org/10.1089/ars.2011.3974> (2011).
32. Merzetti, E. M. & Staveley, B. E. Spargel, the PGC-1 α homologue, in models of Parkinson disease in *Drosophila melanogaster*. *BMC Neurosci.* **16**, 70. <https://doi.org/10.1186/s12868-015-0210-2> (2015).
33. Zhang, X. et al. Alogliptin prevents diastolic dysfunction and preserves left ventricular mitochondrial function in diabetic rabbits. *Cardiovasc. Diabetol.* **17**(1), 160. <https://doi.org/10.1186/s12933-018-0803-z> (2018).
34. Son, R. H. et al. Potential of lycii radices cortex as an ameliorative agent for skeletal muscle atrophy. *Pharmaceuticals (Basel)* **17**(4), 462. <https://doi.org/10.3390/ph17040462> (2024).
35. Song, J. H. et al. Hydroethanolic extract of *Cirsium setidens* ameliorates doxorubicin-induced cardiotoxicity by AMPK-PGC-1 α -SOD-mediated mitochondrial protection. *Phytomedicine* **129**, 155633. <https://doi.org/10.1016/j.phymed.2024.155633> (2024).
36. Diop, S. B. et al. PGC-1/spargel counteracts high-fat-diet-induced obesity and cardiac lipotoxicity downstream of TOR and brummer ATGL lipase. *Cell. Rep.* **10**(9), 1572–1584. <https://doi.org/10.1016/j.celrep.2015.02.022> (2015).
37. Gu, S. C. et al. Myricetin mitigates motor disturbance and decreases neuronal ferroptosis in a rat model of Parkinson's disease. *Sci. Rep.* **14**(1), 15107. <https://doi.org/10.1038/s41598-024-62910-6> (2024).
38. Liu, D. et al. Effects of exercise intervention on type 2 diabetes patients with abdominal obesity and low thigh circumference (EXTEND): study protocol for a randomized controlled trial. *Front. Endocrinol. (Lausanne)* **13**, 937264. <https://doi.org/10.3389/fendo.2022.937264> (2022).
39. Kotake, H. et al. Endurance Exercise training-attenuated diabetic kidney disease with muscle weakness in spontaneously diabetic torii fatty rats. *Kidney Blood Press. Res.* **47**(3), 203–218. <https://doi.org/10.1159/000521464> (2022).
40. Wen, D. T., Wang, W. Q., Hou, W. Q., Cai, S. X. & Zhai, S. S. Endurance exercise protects aging *Drosophila* from high-salt diet (HSD)-induced climbing capacity decline and lifespan decrease by enhancing antioxidant capacity. *Biol. Open* **9**(5), bio045260. <https://doi.org/10.1242/bio.045260> (2020). Published 2020 May 29.
41. Peng, T. et al. Exercise training upregulates cardiac mtp expression in *Drosophila melanogaster* with HFD to improve cardiac dysfunction and abnormal lipid metabolism. *Biology (Basel)* **11**(12), 1745. <https://doi.org/10.3390/biology11121745> (2022).
42. Reisman, E. G., Hawley, J. A. & Hoffman, N. J. Exercise-regulated mitochondrial and nuclear signalling networks in skeletal muscle. *Sports Med.* **54**(5), 1097–1119. <https://doi.org/10.1007/s40279-024-02007-2> (2024).
43. Xie, X. & Huang, C. Role of the gut-muscle axis in mitochondrial function of ageing muscle under different exercise modes. *Ageing Res. Rev.* **98**, 102316. <https://doi.org/10.1016/j.arr.2024.102316> (2024).
44. Matsukawa, T. et al. Upregulation of skeletal muscle PGC-1 α through the elevation of cyclic AMP levels by Cyanidin-3-glucoside enhances exercise performance. *Sci. Rep.* **7**, 44799. <https://doi.org/10.1038/srep44799> (2017).
45. Das, S., Kumar, P., Verma, A., Maiti, T. K. & Mathew, S. J. Myosin heavy chain mutations that cause Freeman–Sheldon syndrome lead to muscle structural and functional defects in *Drosophila*. *Dev. Biol.* **449**(2), 90–98. <https://doi.org/10.1016/j.ydbio.2019.02.017> (2019).
46. Tinkerhess, M. J. et al. The *Drosophila* PGC-1 α homolog spargel modulates the physiological effects of endurance exercise. *PLoS ONE* **7**(2), e31633. <https://doi.org/10.1371/journal.pone.0031633> (2012).

47. Damschroder, D. et al. Stimulating the sir2-spergel axis rescues exercise capacity and mitochondrial respiration in a *Drosophila* model of Barth syndrome. *Dis. Model. Mech.* **15**(10), dmm049279. <https://doi.org/10.1242/dmm.04927> (2022).
48. Al-Horani, R. A., Janaydeh, S., Al-Trad, B., Aljanabi, M. M. & Muhaidat, R. Acute exercise promptly normalizes myocardial myosin heavy-chain isoform mRNA composition in diabetic rats: implications for diabetic cardiomyopathy. *Medicine (Kaunas)* **59**(12), 2193. <https://doi.org/10.3390/medicina59122193> (2023).
49. Gao, Y. H., Wen, D. T., Du, Z. R., Wang, J. F. & Wang, S. J. Muscle psn gene combined with exercise contribute to healthy aging of skeletal muscle and lifespan by adaptively regulating Sirt1/PGC-1 α and arm pathway. *PLoS ONE* **19**(5), e0300787. <https://doi.org/10.1371/journal.pone.0300787> (2024).
50. Joassard, O. R. et al. Regulation of Akt-mTOR, ubiquitin-proteasome and autophagy-lysosome pathways in response to formoterol administration in rat skeletal muscle. *Int. J. Biochem. Cell. Biol.* **45**(11), 2444–2455. <https://doi.org/10.1016/j.biocel.2013.07.019> (2013).

Acknowledgements

We thank the Core Facility of *Drosophila* Resource and Technology, Center for Excellence in Molecular Cell Science, Chinese Academy of Sciences for providing fly stocks and reagents.

Author contributions

Xinyuan Yin wrote the initial draft and conducted experimental data analysis, Dengtai Wen received funding support and revised the article, Hanyu Li assisted in data analysis, Zhaoqing Gao assisted in data analysis, Yuze Gao assisted in the experiment, and Weijia Hao assisted in the experiment.

Funding

Shandong Province Higher Education Youth Innovation Team Project (2023RW057), National Natural Science Foundation of China (NSFC) (No. 32000832).

Declarations

Competing interests

The authors declare no competing interests.

Additional information

Supplementary Information The online version contains supplementary material available at <https://doi.org/10.1038/s41598-024-79415-x>.

Correspondence and requests for materials should be addressed to X.-y.Y. or D.-t.W.

Reprints and permissions information is available at www.nature.com/reprints.

Publisher's note Springer Nature remains neutral with regard to jurisdictional claims in published maps and institutional affiliations.

Open Access This article is licensed under a Creative Commons Attribution-NonCommercial-NoDerivatives 4.0 International License, which permits any non-commercial use, sharing, distribution and reproduction in any medium or format, as long as you give appropriate credit to the original author(s) and the source, provide a link to the Creative Commons licence, and indicate if you modified the licensed material. You do not have permission under this licence to share adapted material derived from this article or parts of it. The images or other third party material in this article are included in the article's Creative Commons licence, unless indicated otherwise in a credit line to the material. If material is not included in the article's Creative Commons licence and your intended use is not permitted by statutory regulation or exceeds the permitted use, you will need to obtain permission directly from the copyright holder. To view a copy of this licence, visit <http://creativecommons.org/licenses/by-nc-nd/4.0/>.

© The Author(s) 2024